frontiers | Frontiers in Physics

ORIGINAL RESEARCH
published: 15 July 2022
doi: 10.3389/fphy.2022.944705

Enhanced Performance of the 4 × 20 Gbit/s-40 GHz OFDM-Based RoFSO Transmission Link Incorporating WDM-MDM of Hermite Gaussian and Laguerre Gaussian Modes

Karamjeet Singh[1], Mehtab Singh[2], Amit Grover[1], Rajan Miglani[3], Harjeevan Singh[2] and El Mehdi Amhoud[4]**

[1]Department of Electronics and Communication Engineering, Shaheed Bhagat Singh State University, Ferozepur, India, [2]Department of Electronics and Communication Engineering, University Institute of Engineering, Chandigarh University, Mohali, India, [3]School of Electronics and Electrical Engineering, Lovely Professional University, Phagwara, India, [4]School of Computer Science, Mohammed VI Polytechnic University, Benguerir, Morocco

OPEN ACCESS

Edited by:
Muhammad Saadi,
University of Central Punjab, Pakistan

Reviewed by:
A. K. M. Sharoar Jahan Choyon,
University of New Mexico,
United States
Sergio Sombra,
Federal University of Ceara, Brazil

***Correspondence:**
Rajan Miglani
rajanmiglani1028@gmail.com
El Mehdi Amhoud
elmehdi.amhoud@um6p.ma

Specialty section:
This article was submitted to
Optics and Photonics,
a section of the journal
Frontiers in Physics.

Received: 15 May 2022
Accepted: 01 June 2022
Published: 15 July 2022

Citation:
Singh K, Singh M, Grover A, Miglani R,
Singh H and Amhoud EM (2022)
Enhanced Performance of the 4 ×
20 Gbit/s-40 GHz OFDM-Based
RoFSO Transmission Link
Incorporating WDM-MDM of Hermite
Gaussian and Laguerre
Gaussian Modes.
Front. Phys. 10:944705.
doi: 10.3389/fphy.2022.944705

A 4 × 20 Gbit/s-40 GHz orthogonal frequency-division multiplexing-based radio-on-free-space optics information link, integrating hybrid wavelength- and mode-division multiplexed transmission techniques, is proposed in this paper. Furthermore, an ameliorated detection scheme deploying a square root module after each photo diode at the receiver terminal is proposed to mitigate the adverse performance effects because of nonlinear photodiode characteristics. The presented results show a successful 80 Gbit/s-160 GHz transmission at 3000 and 2700 m under heavy rainy and foggy weather, respectively. The link demonstrates superior performance in terms of maximum range and transmission rate compared to previous works.

Keywords: RoFSO, weather attenuation, multiplexing, transmission range, OFDM

1 INTRODUCTION

The exponential rise in the number of mobile service users and the services having high bandwidth consumption such as HDTV, networking websites, video-conferencing, and cloud computing, have led to an unparalleled demand in channel bandwidth [1–3]. According to the Cisco Visual Networking Index [4], the global mobile traffic density is expected to increase tenfold from 2015 to 2020. Radio-on-free-space optics (RoFSO) transmission is a cutting-edge data transmission technology for sharing real-time data securely, effectively, and reliably, irrespective of time and geographical area [5]. In RoFSO links, the costly equipment used for different signal processing stages including data encoding and decoding, up- and down-conversion of signal frequency, channel multiplexing and de-multiplexing, and hands-off are jointly shared with the base transceiver, which minimizes the effective cost in the implementation of information transportation [6]. Other merits include last-mile access in rural and remote areas, no security upgrade requirements, no costly fiber deployments and installation on building rooftops, and so on [7]. However, factors such as signal absorption, scattering, scintillation, deep fades, and weather conditions degrade the RoFSO link performance [8]. In temperate regions, heavy rainfall is the most prominent weather condition that adversely affects the performance of RoFSO links [9]. Fog is a crucial weather

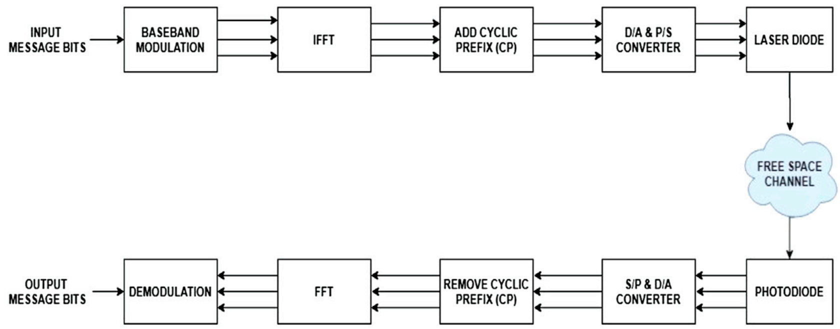

FIGURE 1 | Conceptual schematic of OFDM-FSO transmission.

phenomenon adversely affecting the RoFSO transmission because the fog particle size is comparable to the carrier-wavelength used in RoFSO transmission.

Optical orthogonal frequency-division multiplexing (OFDM) is a subset of multicarrier modulation where the high-speed information bits are transported over many low-speed sub-carriers [10, 11]. When implemented with RoFSO transmission, OFDM results in a low-power consuming and cost-effective information transmission system with enhanced performance [7]. In OFDM, a high-bit-rate information stream is divided into many low-bit-rate streams transported simultaneously. The main objective of implementing the OFDM technique is to lower the baud rate so that the system provides high tolerance to channel effects and deep fades that degrade the performance of the RoFSO transmission link. The integration of the OFDM technique with RoFSO links will explore the combined merits of both technologies to emerge as a viable solution in providing last-mile access for broadband connectivity [14]. The merits of hybrid OFDM-RoFSO technology include 1) high-speed links, 2) elimination of inter-symbol interference (ISI), 3) improvement of signal-to-noise ratio (SNR), 4) ability to cope with frequency selective fading, 5) high spectral efficiency, and 6) robustness against co-channel interference [15].

Figure 1 illustrates the conceptual schematic of the OFDM-FSO transmission. The input message bits are modulated employing M-ary schemes such as phase-shift keying (PSK) and quadrature amplitude modulation (QAM). The narrowband sub-carriers are more robust to signal fading than the high-bit-rate signal and do not require any equalization. These narrowband bit streams are then OFDM modulated using the inverse fast Fourier transformation (IFFT) algorithm, and then the cyclic prefix is added to this signal. It is then followed by digital-to-analog (D/A) conversion and parallel-to-serial (P/S) conversion. The signal is then modulated over a continuous wave laser diode and then propagated over free-space channel. At the input of receiver, a photo diode is deployed, which converts the input optical beam to electrical signal, and the reverse process is executed to recover the message signal.

Recently, investigation of OFDM-based FSO links has been reported in many works. Thus, Zhou et al. exploited OFDM-based FSO transmission using a 16-level PSK modulation scheme [16]. Further, the proposed FSO link is investigated for complex atmospheric weather phenomenon viz. sunny, rainy, snowy, and foggy states. The simulation analysis of the link demonstrates reliable high-speed transmission at 500 m FSO range with BER of $10^{-4.2}$ and clear constellation plots. In another work reported by Jaiswal et al. [17], an M-ary QAM based OFDM-FSO link was investigated under weak and strong turbulence conditions. The authors compared the performance of 64-level, 128-level, and 256-level QAM schemes. The results indicate that the 64-level QAM shows better performance, and the link shows reliable transportation of data at the 7000 m FSO range. Kumar et al. reported a non-line-of-sight configuration-based OFDM-FSO link using multi-hop relay [18]. Analog network coding has been incorporated to provide enhanced throughput, power efficiency, and BER performance of the link. The incorporation of coherent detection technique in an OFDM-based FSO transmission is explored in [19]. 128 and 512 sub-carrier transmissions were compared, and results indicated that the SNR performance of the link improves by 6 dB on increasing the number of sub-carriers. Further, on investigating the link for varying atmospheric turbulence, the results indicated that the received signal was more degraded for strong turbulence conditions. Dabiri et al. compared the 4-level, 16-level, and 64-level QAM transmission in an OFDM-based FSO link under varying turbulence levels and demonstrated that 4-QAM was a better choice for modulation scheme when designing a high-speed FSO link under strong turbulence conditions [20].

Wavelength division multiplexing (WDM) is an important technology in which multiple data signals are transported simultaneously over the same channel using different optical beams from distinct laser source to realize a high-speed information transmission link [21, 22]. **Figure 2** illustrates the conceptual block diagram of the WDM-based FSO link.

In WDM systems, multiple information signals from different transmitter sections each using a distinct laser source are combined using a WDM multiplexer (MUX), and then the multiplexed signal is transmitted through free-space channel. Independent signals at the receiver are demultiplexed by employing a WDM de-multiplexer (DEMUX) and a dedicated receiver section demodulates each signal. Shat et al. explored a 3-channel WDM-FSO transmission in which each channel transports 2.5 Gbit/s signals [25]. The transmission is

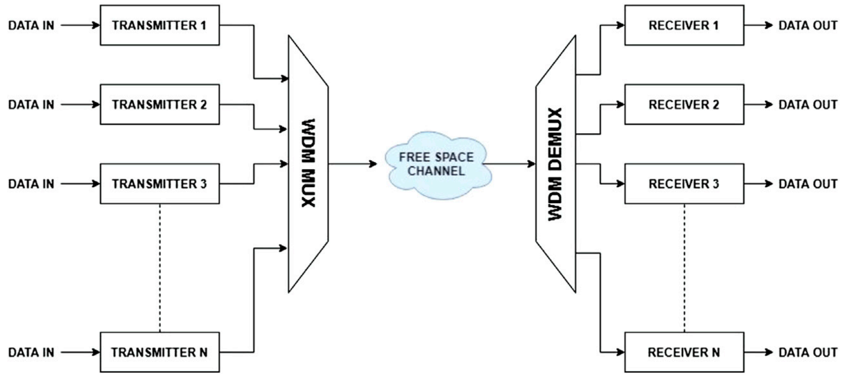

FIGURE 2 | Conceptual diagram of WDM-based FSO link.

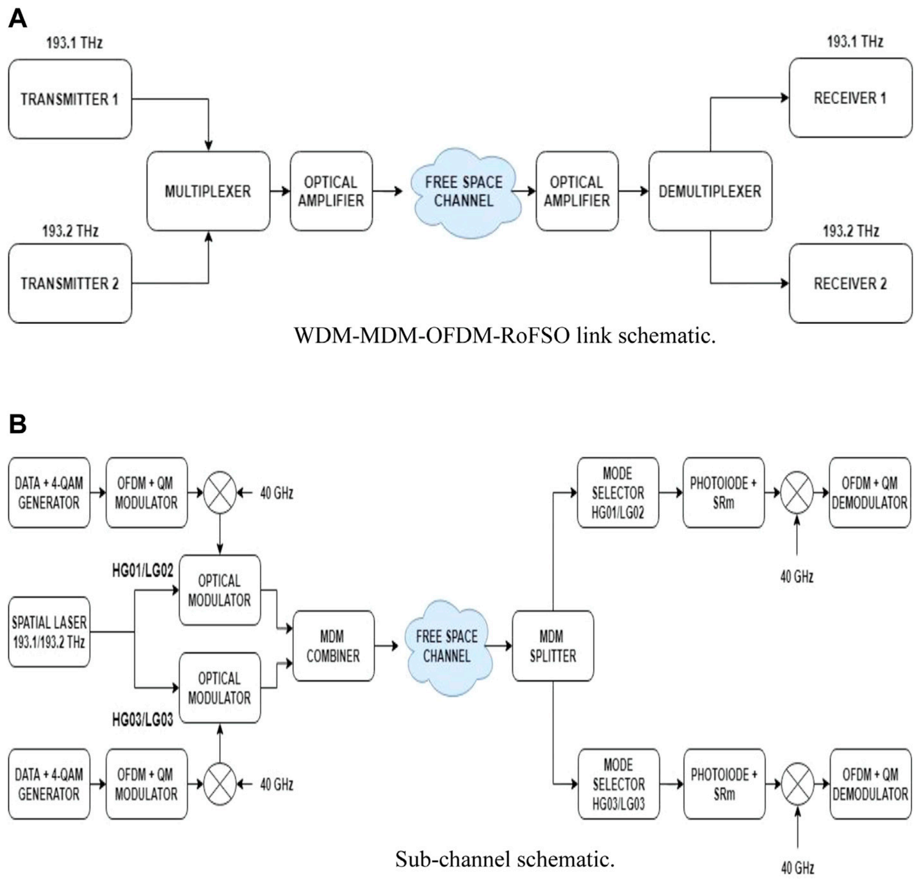

FIGURE 3 | (A) WDM-MDM-OFDM-RoFSO link schematic. **(B)** sub-channel schematic.

investigated for light, medium, and heavy rainy conditions, and maximum achievable range is computed as 15.6, 6.1, and 3 km, respectively. Robinson et al. reported a hybrid course wavelength division multiplexed (CWDM)- and dense wavelength division multiplexed (DWDM)-based FSO link in which 4 CWDM and 12 DWDM channels, each carrying 2.5 Gbit/s information, were transported over a free-space channel [26]. The simulation results demonstrate a reliable 30 Gbit/s transmission at 2.04 km FSO range for heavy foggy and 2.64 km FSO range for heavy rainy conditions. Jain et al. reported performance comparison of return-to-zero and non-return-to-zero modulation schemes in a DWDM-based FSO link at different optical transmission bands viz. S, C, and L band [27]. The performance of the link was investigated at the 10 Gbit/s transmission rate, and non-return-

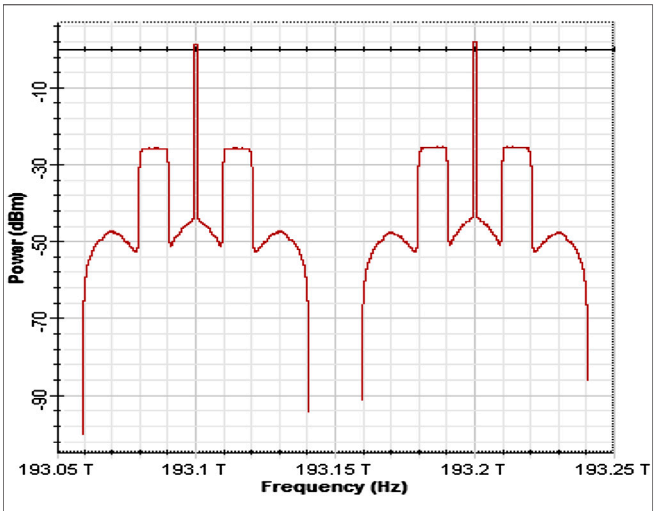

FIGURE 4 | Optical spectrum of the transmitted signal.

to-zero at C-band was proved to be an optimal choice for implementing DWDM systems. The BER performance analysis of a 4-channel WDM-based FSO link by using the spectrum slicing technique is discussed in [28]. 4 × 1.56 Gbit/s data transmission for different climate phenomena of Vellore city in India have been discussed. The results reported reliable transmission of all channels at 3.3 km for heavy rainy and 2.7 km for heavy foggy conditions. Furthermore, Huang et al. explored a WDM-FSO transmission where 4-channels were transported over free-space at hybrid data transmission rates using a doublet lens scheme [29]. The authors report reliable transmission of 10 Gbit/s, 25 Gbit/s, 28 Gbit/s, and 32 Gbit/s data signals over the 100 m FSO range. The scheme was proposed for implementing light-based low-cost high-speed WiFi applications.

Mode division multiplexing (MDM) is a novel technique that has emerged as a cost-effective solution for providing high-speed optical communication links [30, 31]. In MDM systems, the transmission capacity is enhanced by capitalizing Eigen mode dimension of the laser beam for parallel transportation of multiple information streams. Rjeb et al. reported the development and performance investigation of MDM of orbital angular momentum (OAM) beams with the vortex of order $l = \pm 2$ in a few mode fiber based on inverse raised cosine function for improved performance [32]. Rusch et al. explored the transmission of three quadrature PSK modulated OAM beam with $l = 0, -1, and + 1$ over the 1.4 km ring core fiber with minimum crosstalk using 2 × 2 MIMO processor [33].

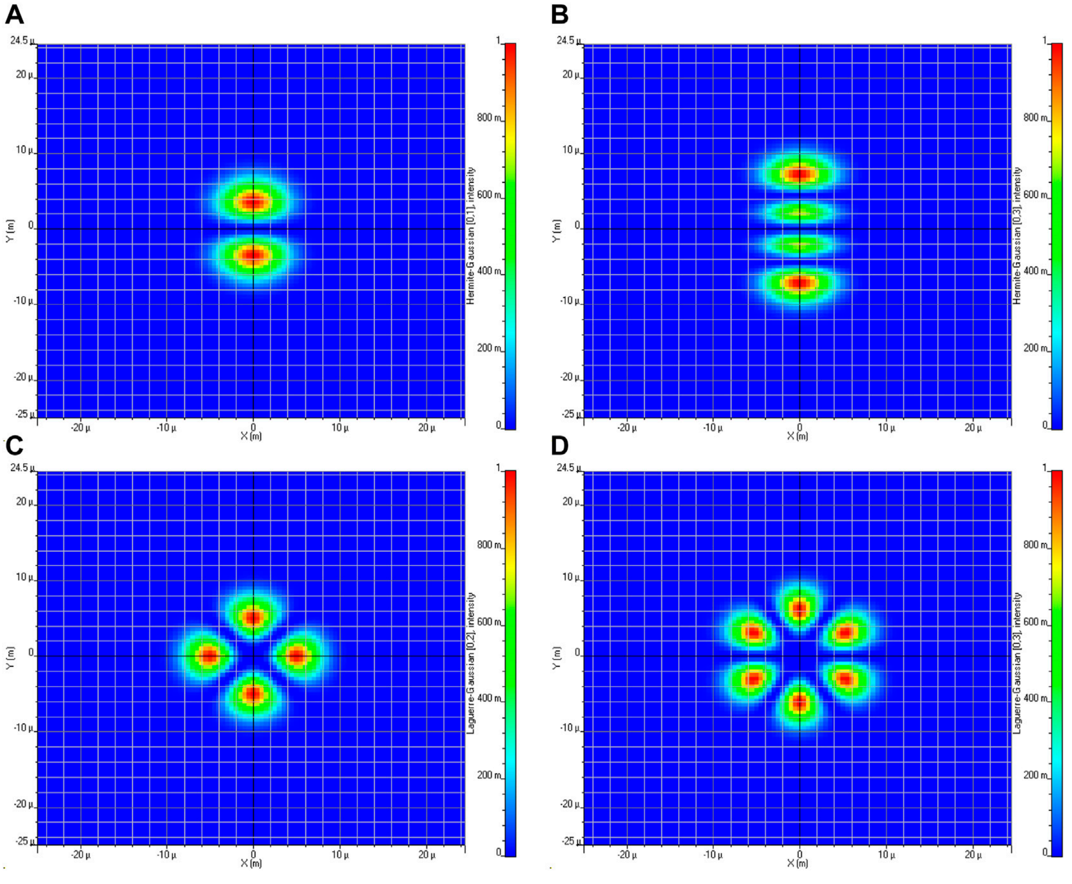

FIGURE 5 | Spatial profiles of **(A)** HG01, **(B)** HG03, **(C)** LG02, and **(D)** LG03 modes.

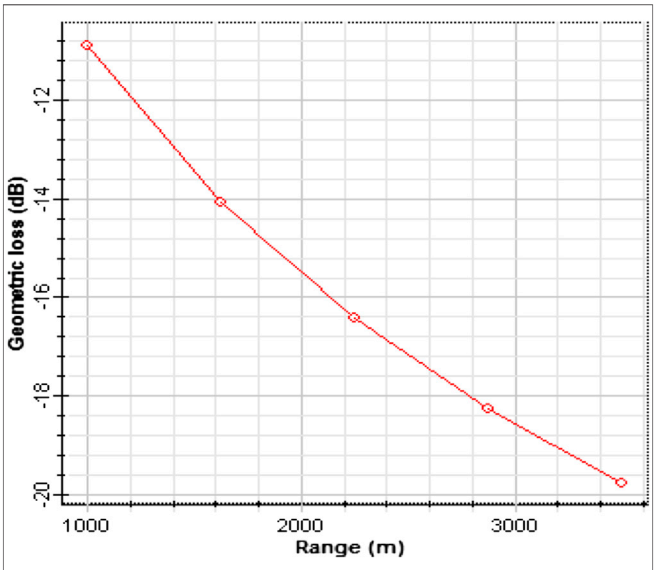

FIGURE 6 | Geometrical loss vs. range.

TABLE 1 | Dependence of rainfall rates on visibility [66].

Weathexr	Rainfall Rate	Visibility
Light rainy weather	0.25 mm/h	18–20 km
Moderate rainy weather	12.5 mm/h	2.8–10 km
Heavy rainy weather	25 mm/h	1.9–2 km

Likewise, fog attenuation can be modeled as [67].

Further, 4 independent 16-level QAM modulated channels using linear polarized beams are transported over 0.9 km elliptical ring core fiber. M. Hussain et al. explored the designing and investigation of a novel photonic crystal fiber that can transport up to 26 OAM beams simultaneously with low crosstalk for high-speed MDM applications [34]. The work in [35] reported 40 Gbit/s 4-OAM beam transmission under various FSO weather conditions. The works in [36, 37] report investigations on the impact of climate conditions on MDM-based FSO links. Furthermore, the application of FSO links for inter-satellite data transportation, photonic radar applications, and 5G services is reported in [41, 42].

Polarization division multiplexing (PDM) is another important technique that enhances the transmission capacity and spectral efficiency of optical links. The authors in [60] reported and investigated 640 Gbit/s hybrid PDM-WDM-based FSO transmission under adverse climate conditions of Bangladesh. A 320 Gbit/s hybrid PDM-WDM-based FSO transmission incorporating the AMI encoding scheme under adverse climate conditions was discussed in [61]. The investigations on a binary PSK RF-subcarrier FSO system using coherent detection under strong turbulence conditions has been reported in [62]. The performance comparison of on/off keying, binary, differential, quadrature, and 8-level PSK under the effect of strong atmospheric turbulent conditions is reported in [63]. The application of circular PDM with coherent detection OFDM transmission in FSO for enhanced performance was reported in [64].

Here, we present the designing of the 80 Gbit/s-160 GHz RoFSO link using hybrid WDM-MDM-OFDM techniques with enhanced detection and investigate the proposed link for heavy rainy and foggy weather. **Section 2** elucidates link schematic, results are discussed in **Section 3** followed by the concluding remarks in **Section 4**.

2 LINK SCHEMATIC

The schematic of WDM-MDM-OFDM-RoFSO link is elucidated **Figure 3**. Opti-System and MATLAB tools were used to implement this work.

At 193.1 THz central frequency, HG01 transports channel 1 data, and HG03 transports channel 2 data. Likewise, at 193.2 THz, LG02 transports channel 3 data and LG03 transports channel 4 data. A multiplexer combines both frequency channels. **Figure 4** elucidates the spectrum of the transmitted signal. **Figure 5** shows the excited profiles of HG and LG modes at the transmitter terminal.

The HG and LG modes are mathematically described using **Eqs. 1**, **2** respectively as [36]:

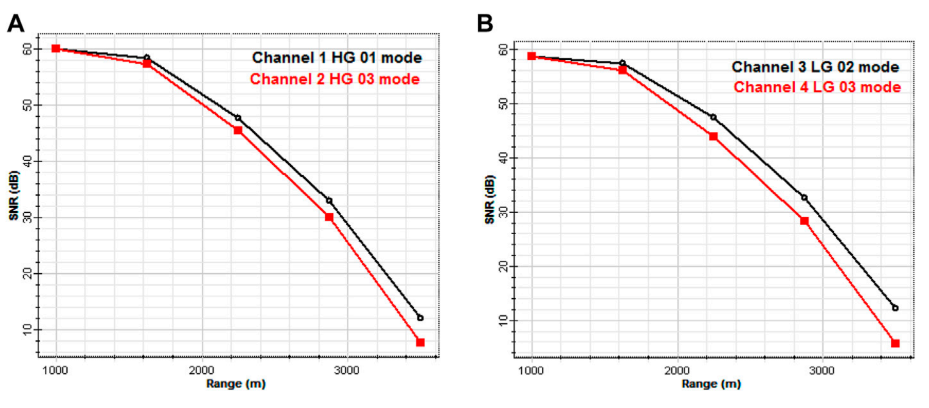

FIGURE 7 | SNR vs. Range for **(A)** channel 1 and 2 **(B)** channel 3 and 4 for heavy rain conditions.

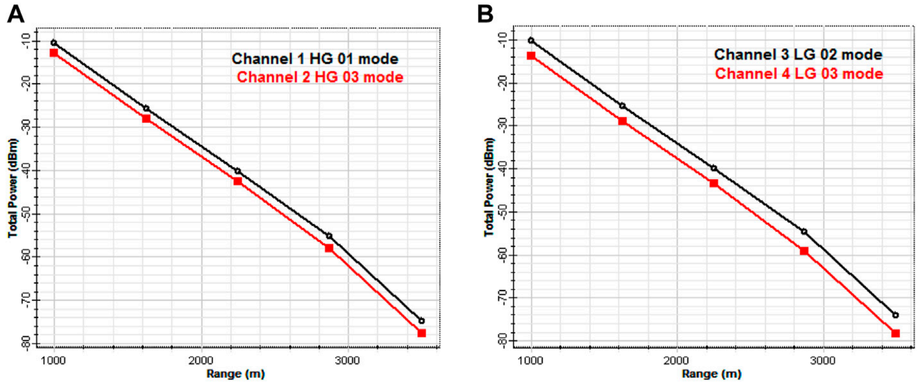

FIGURE 8 | Power vs. Range for **(A)** channel 1 and 2 **(B)** channel 3 and 4 for heavy rain conditions.

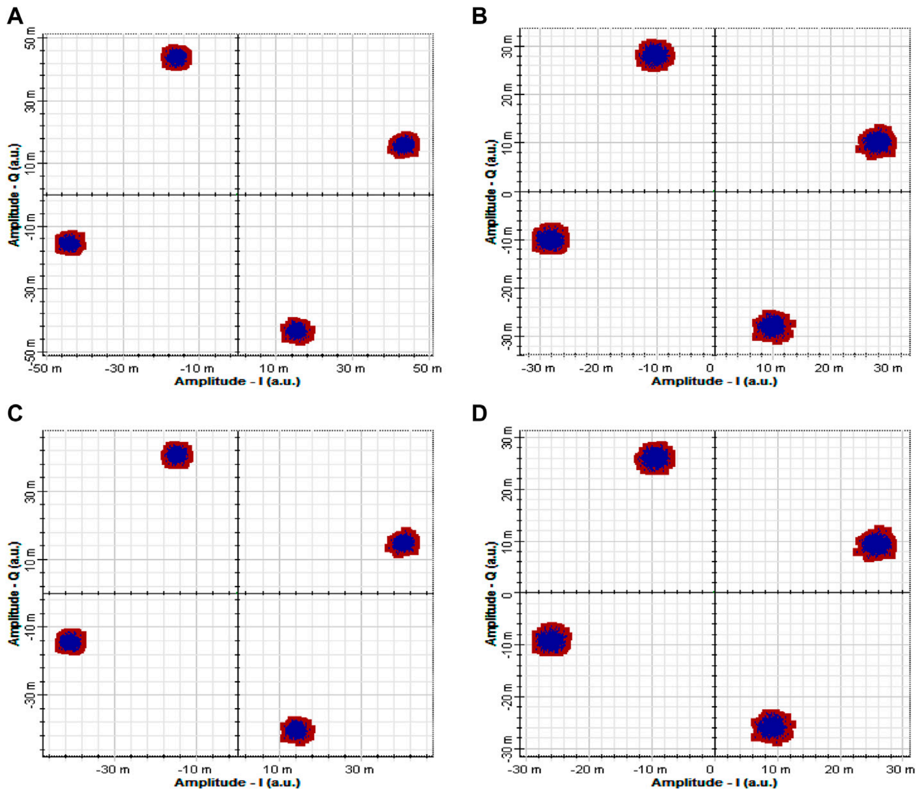

FIGURE 9 | Constellation graph at 3000 m range for **(A)** channel 1, **(B)** channel 2, **(C)** channel 3, and **(D)** channel 4 under heavy rainy conditions.

$$\varphi_{m,n}(x, y) = H_m\left(\frac{\sqrt{2}x}{\omega_{0,x}}\right)\exp\left(-\frac{x^2}{\omega_{ox}^2}\right)\exp\left(j\frac{\pi x^2}{\lambda R_{ox}}\right) \times H_n\left(\frac{\sqrt{2}y}{w_{o,y}}\right)\exp\left(-\frac{y^2}{w_{oy}^2}\right) \times \left(j\frac{\pi y^2}{\lambda R_{oy}}\right), \quad (1)$$

$$\varphi_{m,n}(r, \varnothing) = \left(\frac{2r^2}{w_o^2}\right)^{|n/2|} L_m^n\left(\frac{2r^2}{w_0^2}\right)\exp\left(\frac{r^2}{w_0^2}\right) \times \exp\left(j\frac{\pi r^2}{\lambda R_0}\right) \times \left\{\begin{array}{l} \sin(|n|\varnothing),\ n \geq 0 \\ \cos(|n|\varnothing),\ n < 0 \end{array}\right\}, \quad (2)$$

where the$X$-polarization axis modal dependency is denoted by m, the Y-polarization axis modal dependency is denoted by n, the Laguerre polynomial is denoted by L_m^n, and the Hermite polynomials

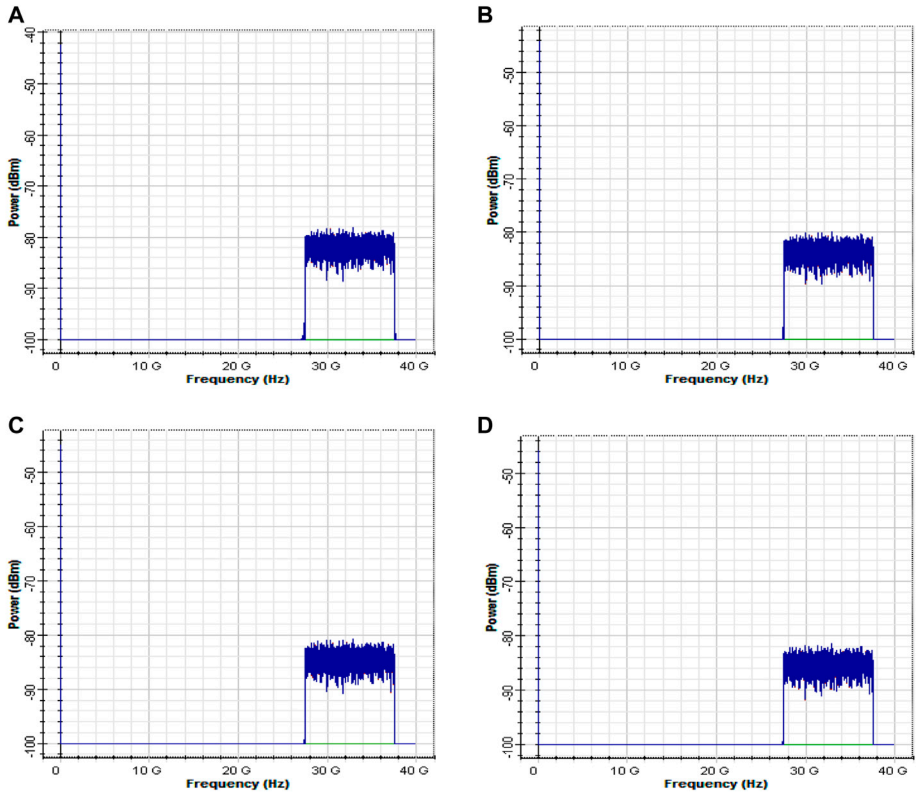

FIGURE 10 | RF power at the 3000 m range for **(A)** channel 1, **(B)** channel 2, **(C)** channel 3, and **(D)** channel 4 under heavy rainy conditions.

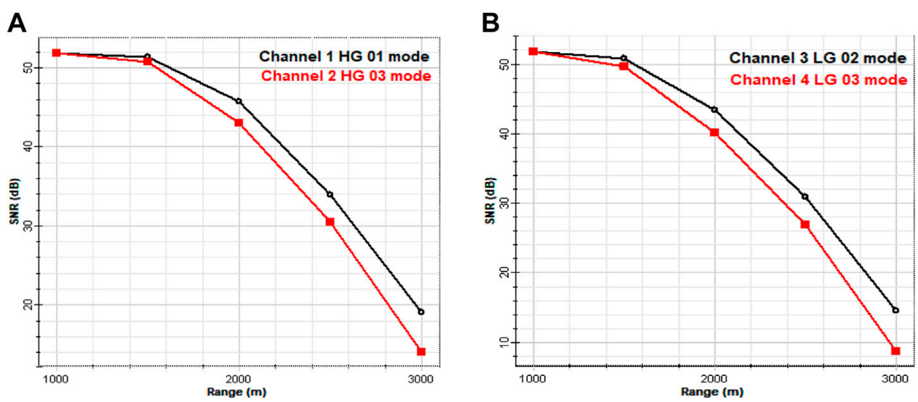

FIGURE 11 | SNR vs. range for **(A)** channel 1 and 2 **(B)** channel 3 and 4 for heavy foggy conditions.

are denoted by H_m and H_n, and the radius of beam and spot size are denoted by R and w_0, respectively. 20 Gbit/s 4-level QAM signals having 2-bits per symbol are OFDM modulated using 32 prefix points, 512 sub-carriers, and 1024 IFFT points. This signal is mixed with the 7.5 GHz quadrature modulator (QM) at 40 GHz and then transmitted into the free-space channel modeled as [36]:

$$P_{Received} = P_{Transmitted}\left(\frac{d_R^2}{(d_T + \theta Z)^2}\right)10^{-\sigma Z/10}, \quad (3)$$

where the optical power at the photodetector surface is denoted by $P_{Received}$, transmitted optical power is denoted by $P_{Transmitted}$, the diameter of receiver and transmitter antenna is represented by d_R and d_T, respectively, range is represented by Z, and weather attenuation by σ. The simulation parameters have been considered as per practical RoFSO links reported in [36–40]. Optical amplifier with 12 dB gain has been deployed for enhancing the link range. Different modes at the receiver side are separated using mode selector and the spatial modes are

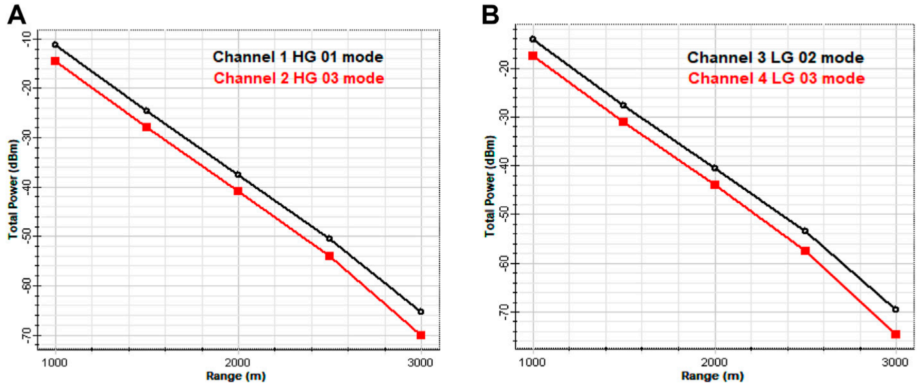

FIGURE 12 | Power vs. range for **(A)** channel 1 and 2 **(B)** channel 3 and 4 for heavy foggy conditions.

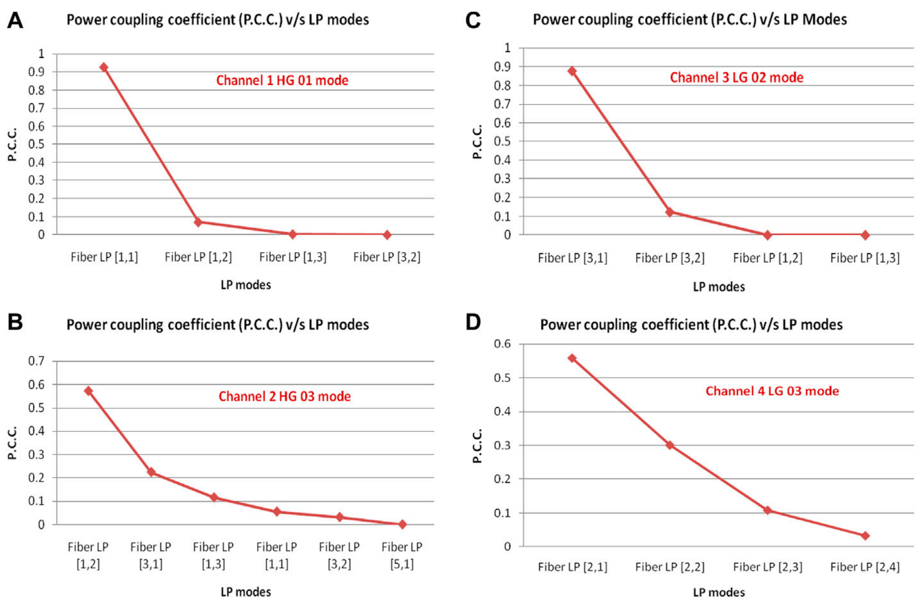

FIGURE 13 | Modal decomposition analysis of **(A)** channel 1 HG01 mode **(B)** channel 2 HG03 mode **(C)** channel 3 LG02 mode **(D)** channel 4 LG03 mode.

converted to electrical signal using photodiode. A square root module (SRm) is used after the photo diode to compensate for its nonlinear response. The transmitted message is recovered using the QAM demodulator preceding OFDM and QM decoders. Attenuation for varying levels of rainy weather can be calculated using the equation [65]:

$$\beta_{\text{rain}} = 1.076R^{0.67}, \tag{4}$$

where R is the rainfall rate in mm/hr. The attenuation because of rainy weather in RoFSO links can be reasonably approximated by having information about the visibility range, V (km) (**Table 1**) as:

$$\sigma_{\text{rain}} = \frac{2.8}{V}, \tag{5}$$

$$\beta_{fog}(\lambda) = \frac{3.91}{V}\left(\frac{\lambda}{550}\right)^{-p}, \tag{6}$$

where λ (nm) is the optical beam wavelength, and p is the scattering coefficient, which is expressed using Kim's model as [68]:

$$p = \begin{cases} 1.6 & V > 50 \\ 1.3 & 6 < V < 50 \\ 0.16V + 0.34 & 1 < V < 6 \\ V - 0.5 & 0.5 < V < 1 \\ 0 & V < 0.5 \end{cases}, \tag{7}$$

Based on the above equations, the attenuation for heavy rainy and foggy weather is approximated to be 19.28 and 22 dB/km,

TABLE 2 | The comparison of the system performance with conventional techniques reported in literature [26, 28, 70–81].

Author/Ref	Method	Data Rate	Atmospheric Condition	Link Range (km)
Robinson S et al. Reference [26]	Hybrid DWDM + CWDM	12 λ × 2.5 Gbit/s	Heavy rain	2.64
			Heavy fog	2.04
Prabhu K et al. Reference [28]	Spectrum-slicing-based WDM	4 λ × 1.56 Gbit/s	Heavy rain	3.3
			Heavy fog	2.7
Hatim S et.al. Reference [70]	WDM	16 λ × 2.5 Gbit/s	Heavy rain	2.4
Gailani S et.al. References [71, 72]	Multibeam concept	1 Gbit/s	Heavy rain	1.14
Gailani S et.al. References [73, 74]	Hybrid WDM-Multibeam concept	4 λ × 1.25 Gbit/s	Heavy rain	1.09
Sahu N et.al. Reference [75]	Hybrid WDM-Multibeam concept	16 λ × 2.5 Gbit/s	Heavy rain	2.54
Robinson S et.al. Reference [76]	Hybrid CWDM-Multibeam concept	12 λ × 2.5 Gbit/s	Heavy rain	3
			Heavy fog	2.35
Kumar N et.al. Reference [77]	OFDM	10 Gbit/s	Heavy rain	0.6
			Heavy fog	0.1
Dayal N et.al. Reference [78]	WDM with hybrid optical amplifier	3 λ × 2.5 Gbit/s	Heavy rain	5
Kaur G. et.al. Reference [79]	SAC-OCDMA with DDW code	5 Gbit/s	Heavy rain	1
Sharma V et.al. Reference [80]	CO-CDMA with OSSB signal	10 Gbit/s	Heavy rain	1
			Heavy fog	0.48
Kakati D et.al. Reference [81]	DP-16-QAM with DSP	120 Gbit/s	Heavy rain	1
			Heavy fog	0.4
In this work	Hybrid WDM-MDM-OFDM techniques	80 Gbit/s	Heavy rain	3
			Heavy fog	2.7

respectively [68]. Another factor is geometric loss (A_{Geo}) that degrades the RoFSO link performance and is expressed as [69]:

$$A_{Geo} = 10\log_{10}\left[\frac{4A_{RX}}{\pi(\theta Z)^2}\right]\cdot dB, \tag{8}$$

where the area of the surface of receiver antenna is expressed as A_{RX}, the size of laser beam is expressed as θ, and the range is expressed as Z. **Figure 6** reports the geometric loss for the 1000–3500 m FSO range.

3 RESULTS AND DISCUSSION

Figures 7 and **8** report the SNR and power plots at the photo diode for varying range under heavy rainy weather. It is observed from **Figure 7** that the SNR for channel 1 (HG01 mode) is 60.00, 47.69, and 12.14 dB at the 1000, 2250, and 3500 m range, respectively, whereas the SNR for channel 2 (HG03 mode) is 59.98, 45.35, and 7.61 dB at the 1000, 2250, and 3500 m range, respectively. Likewise, the SNR for channel 3 (LG02 mode) is 58.66, 47.30, and 12.04 dB and for channel 4 (LG03 mode) is 58.65, 43.86, and 5.66 dB at the 1000, 2250, and 3500 m range, respectively. The results show that channel 1 (HG01 mode) having the highest SNR at the receiver terminal is most robust against fading followed by channel 3 (LG02 mode), channel 2 (HG03 mode), and channel 4 (LG03 mode). In addition, all the channels are transported reliably at the 3000 m range with acceptable SNR at the receiver (~20 dB). Alternatively, it is observed from **Figure 8** that total power for channel 1 is −10.29, −39.98, and −74.19 dBm; for channel 2 is −12.91, −42.64, and −77.69 dBm; for channel 3 is −10.55, −40.24, and −74.81 dBm; and for channel 4 is −13.76, −43.50, and −78.31 dBm at 1000, 2250, and 3500 m, respectively. The highest power at the receiver terminal is observed for channel 1. Thus, channel 4 (LG03 mode) is most affected by fading, and channel 1 (HG01 mode) is most robust against it.

Figures 9 and **10** present the constellation graph and RF power for all channels at the 3000 m range. The clear constellation graph for all the channels in **Figure 9** indicates a reliable 80 Gbit/s-160 GHz transmission at 3000 m under heavy rainy weather. The results presented in **Figure 10** show that the highest RF power at the receiver terminal is collected by channel 1, which further demonstrates that channel 1 is least susceptible to channel fading.

Furthermore, the link was investigated for heavy foggy weather, as illustrated in **Figures 11** and **12**. The SNR for channel 1 is 51.84, 45.74, and 19.04 dB; for channel 2 is 51.82, 43.03, and 14.01 dB; for channel 3 is 51.82, 43.34, and 14.57 dB; and for channel 4 is 51.77, 40.15, and 8.64 dB at the 1000, 2000, and 3000 m range, respectively. The total power for channel 1 is −11.23, −37.68, and −65.33 dBm; for channel 2 is −14.46, −40.92, and −70.12 dBm; for channel 3 is −14.11, −40.57, and −69.59 dBm; and for channel 4 is −17.57, −44.07, and −74.69 dBm at the 1000, 2000, and 3000 m range, respectively. The results show reliable transmission of all channels up to the 2700 m range under heavy foggy conditions with acceptable SNR.

Figure 13 shows the power-coupling coefficients of different LP modes decomposed at the receiver terminal. For channel 1, most power is coupled into mode LP [1] followed by LP [1, 2], LP [1, 3], and LP [2, 3]. For channel 2, most power is coupled into LP [1, 2] followed by LP [1, 3], LP [1, 3], LP [2, 3], and LP [1, 5]. For channel 3, most power is coupled into the LP [1, 3] mode followed by LP [2, 3], LP [1, 2], and LP [1, 3]. For channel 4, most power is coupled into the LP [1, 2] mode, followed by LP [2], LP [2, 3], and LP [2, 4]. Further, the comparison of the system performance with conventional techniques reported in literature is listed in **Table 2**.

4 CONCLUDING REMARKS

The present work reports the designing and investigation of a high-speed RoFSO link incorporating hybrid WDM-MDM-OFDM techniques under heavy rainy and foggy conditions. Four channels each carrying the 20 Gbit/s-40 GHz information are successfully transmitted using distinct spatial modes (HG01, HG03, LG02, and LG03) over the 3000 and 2700 m range under heavy rain and foggy weather, respectively, with acceptable performance using an enhanced detection technique involving the use of SRm at the receiver terminal. The proposed 4×20 Gbit/s-40 GHz-based RoFSO link provides a useful platform for future long-reach high-capacity RoFSO transmission links. In future works, the performance of the proposed link will be further improved by incorporating optical code-division multiple access transmission along with adaptive optics and digital signal processing techniques at the receiver.

DATA AVAILABILITY STATEMENT

The original contributions presented in the study are included in the article/supplementary material, and further inquiries can be directed to the corresponding author.

AUTHOR CONTRIBUTIONS

All authors listed have made a substantial, direct, and intellectual contribution to the work and approved it for publication.

REFERENCES

1. Gailani S, Mohammad A, Shaddad R. Evaluation of a 1 Gb/s Free Space Optic System in Typical Malaysian Weather. In: Proceedings of IEEE 3rd International Conference on Photonics; 01-03 October 2012; Pulau Pinang, Malaysia. IEEE (2012). p. 121–4. doi:10.1109/icp.2012.6379839
2. Ramezani A, Noroozi M, Aghababaee M. Analyzing Free Space Optical Communication Performance. *Int J Eng Adv Tech* (2014) 4(1):46–51.
3. Singh J, Kumar N. Performance Analysis of Different Modulation Format on Free Space Optical Communication System. *Optik* (2013) 124(20):4651–4. doi:10.1016/j.ijleo.2013.02.014
4. Cisco. 10th Annual Cisco Visual Networking Index (VNI) Mobile Forecast Projects 70 Percent of Global Population Will Be Mobile Users (2016). Available: https://newsroom.cisco.com/press-release-content articleId= 1741352 (Accessed Sep 10, 2017).
5. Amhoud EM, Chafii M, Nimr A, Fettweis G. OFDM With Index Modulation in Orbital Angular Momentum Multiplexed Free Space Optical Links In: In 2021 IEEE 93rd Vehicular Technology Conference (VTC2021-Spring) IEEE (2021) 1–5. doi:10.1109/VTC2021-Spring51267.2021.9448928
6. Mandal GC, Mukherjee R, Das B, Patra AS. Next-generation Bidirectional Triple-Play Services Using RSOA Based WDM Radio on Free-Space Optics PON. *Opt Commun* (2018) 411:138–42. doi:10.1016/j.optcom.2017.11.033
7. Sharma V, Kaur G. High Speed, Long Reach OFDM-FSO Transmission Link Incorporating OSSB and OTSB Schemes. *Optik* (2013) 124:6111–4. doi:10.1016/j.ijleo.2013.04.100
8. Chandra Mandal G, Mukherjee R, Das B, Sekhar Patra A. Bidirectional and Simultaneous Transmission of Baseband and Wireless Signals over RSOA Based WDM Radio-Over-Fiber Passive Optical Network Using Incoherent Light Injection Technique. *AEU - Int J Elect Commun* (2017) 80:193–8. doi:10.1016/j.aeue.2017.07.030
9. Zhou H, Mao S, Agarwal P. Optical Power Allocation for Adaptive WDM Transmission in Free Space Optics Networks. *Digital Commun Networks* (2014) 1:2677–82. doi:10.1016/j.dcan.2015.09.001
10. Zhang Y, Cui Q, Tao X. *Multi-user MIMO-OFDM Systems and Low-Rate CSI Feedback Channel Capacity Analysis Method*, China: Electronics and Information Technology (2009).
11. Onizawa T, Ohta A, Asai Y. Experiments on FPGA-Implemented Eigenbeam MIMO-OFDM with Transmit Antenna Selection. *IEEE Trans Veh Technol* (2009) 58(3):1281–91. doi:10.1109/tvt.2008.928900
12. Saberinia E, Tang J, Tewfik AH, Parhi KK. Pulsed-OFDM Modulation for Ultrawideband Communications. *IEEE Trans Veh Technol* (2009) 58(2): 720–6. doi:10.1109/tvt.2008.923680
13. Kumar N, Sharma A, Kapoor V. Performance Investigations on WDM Based OFDM-RoF Transmission Links. *J Opt Commun* (2014) 35(2):151–6. doi:10.1515/joc-2014-1001
14. Chaudhary S, Amphawan A, Nisar K. Realization of Free Space Optics with OFDM under Atmospheric Turbulence. *Optik* (2014) 125:5196–8. doi:10.1016/j.ijleo.2014.05.036
15. Shao Y, Wang Y, Chi N. 60-GHz RoF System with Low PAPR 16QAM-OFDM Downlink Using PTS Segmentation. *IEEE Photon Technol Lett* (2013) 25: 855–8. doi:10.1109/lpt.2013.2252425
16. Zhou J, Shao Y, Wang Z, Li C, Zhou Y, Ma W. A 16PSK-OFDM-FSO Communication System under Complex Weather Conditions. *Opj* (2016) 06:131–5. doi:10.4236/opj.2016.68b022
17. Jaiswal I, Sangeetha RG, Suchetha M. Performance of M -ary Quadrature Amplitude Modulation -based Orthogonal Frequency Division Multiplexing for Free Space Optical Transmission. *IET Optoelectronics* (2016) 10(4):156–62. doi:10.1049/iet-opt.2015.0091
18. Kumar P, Thakor S. Performance of OFDM-FSO Link with Analog Network Coding. *Photon Netw Commun* (2017) 35(2):210–24. doi:10.1007/s11107-017-0730-z
19. Saruchi Attri S, Charu Narula C, Sanjiv Kumar S. Performance Analysis of FSO Link Using CO-OFDM under the Effect of Atmospheric Turbulence. *Proc Int Conf Intell Commun Control Devices* (2017) 479:167–72. doi:10.1007/978-981-10-1708-7_18
20. Dabiri MT, Saber MJ, Sadough SMS. BER Performance of OFDM-Based Wireless Services over Radio-On-FSO Links in the Presence of Turbulence and Pointing Errors. In: Proc. of 8th International Symposium on Telecommunications (IST); 27-28 September; Tehran, Iran. London: Intech Open (2016). p. 30–3. doi:10.1109/istel.2016.7881776
21. Kaur H, Singh K, Singh T. Performance Analysis of CO-OFDM-FSO System Using PDM. *SSRG-IJEEE* (2020) 7(3):12–7. doi:10.14445/23488379/ijeee-v7i3p103
22. Singh M. Performance Analysis of WDM-FSO System under Adverse Weather Conditions. *Photon Netw Commun* (2018) 36:1–10. doi:10.1007/s11107-018-0763-y
23. Patnaik B, Sahu PK. Novel QPSK Modulation for DWDM Free Space Optical Communication System. In: Proc. of Annual Wireless and Optical Communication Conference; 25-27 June 2012; London, UK. IEEE (2012). 170–5. doi:10.1109/wiad.2012.6296557
24. Noor N, Naji A, Al-Khateeb W. Performance Analysis of a Free Space Optics Link with Multiple Transmitters/Receivers. *IIUM Eng J* (2012) 13(1):49–58. doi:10.31436/iiumej.v13i1.271
25. Shah D, Kothari D. Optimization of 2.5 Gbps WDM-FSO Link Range under Different Rain Conditions in Ahmedabad. In: Proc. of Annual IEEE India Conference (INDICON); 11-13 December; Pune, India. IEEE (2014). p. 1–4. doi:10.1109/indicon.2014.7030643
26. Robinson S, Jasmine S, Pavithra R. Investigation of Hybrid WDM (DWDM+CWDM) Free Space Optical Communication System. *ICTACT J Commun Tech* (2015) 6(4):1187–92. doi:10.21917/ijct.2015.0174
27. Jain D, Mehra R. Performance Analysis of Free Space Optical Communication System for S, C and L Band. In: Proc. of International Conference on

Computer, Communications and Electronics (Comptelix); 01-02 July 2017; Jaipur, India. IEEE (2017). p. 183–9. doi:10.1109/comptelix.2017.8003961
28. Prabu K, Charanya S, Jain M, Guha D. BER Analysis of SS-WDM Based FSO System for Vellore Weather Conditions. *Opt Commun* (2017) 403:73–80. doi:10.1016/j.optcom.2017.07.012
29. Huang X-H, Li C-Y, Lu H-H, Su C-W, Wu Y-R, Wang Z-H, et al. WDM Free-Space Optical Communication System of High-Speed Hybrid Signals. *IEEE Photon J.* (2018) 10(6):1–7. doi:10.1109/jphot.2018.2881701
30. Singh M, Malhotra J. Performance Comparison of High-Speed Long-Reach Mode Division Multiplexing-Based Radio over Free Space Optics Transmission System Using Different Modulation Formats under the Effect of Atmospheric Turbulence. *Opt Eng* (2019) 58(4):046112–9. doi:10.1117/1.oe.58.4.046112
31. Singh M, Malhotra J. Performance Comparison of M-QAM and DQPSK Modulation Schemes in a 2 × 20 Gbit/s-40 GHz Hybrid MDM-OFDM-Based Radio over FSO Transmission System. *Photon Netw Commun* (2019) 38: 378–89. doi:10.1007/s11107-019-00861-z
32. Rjeb A, Guerra G, Issa K, Fathallah H, Chebaane S, Machhout M, et al. Inverse-raised-cosine Fibers for Next-Generation Orbital Angular Momentum Systems. *Opt Commun* (2019) 458:1–14. doi:10.1016/j.optcom.2019.124736
33. Rusch LA, Larochelle S. Fiber Transmission Demonstrations in Vector Mode Space Division Multiplexing. *Front Optoelectron* (2018) 11(2):155–62. doi:10.1007/s12200-018-0812-2
34. Hassan MM, Kabir MA, Hossain MN, Biswas B, Paul BK, Ahmed K. Photonic crystal Fiber for Robust Orbital Angular Momentum Transmission: Design and Investigation. *Opt Quan Elect* (2019) 52(1):1–8. doi:10.1007/s11082-019-2125-0
35. Singh M, Atieh A, Grover A, Barukab O. Performance Analysis of 40 Gb/s Free Space Optics Transmission Based on Orbital Angular Momentum Multiplexed Beams. *Alexandria Eng J* (2022) 61(7):5203–12. doi:10.1016/j.aej.2021.10.043
36. Chaudhary S, Tang X, Wei X. Comparison of Laguerre-Gaussian and Donut Modes for MDM-WDM in OFDM-Ro-FSO Transmission System. *AEU - Int J Elect Commun* (2018) 93:208–14. doi:10.1016/j.aeue.2018.06.024
37. Chaudhary S, Amphawan A. Solid Core PCF-Based Mode Selector for MDM-Ro-FSO Transmission Systems. *Photon Netw Commun* (2018) 36(2):263–71. doi:10.1007/s11107-018-0778-4
38. Chaudhary S, Amphawan A. Selective Excitation of LG 00, LG 01, and LG 02 Modes by a Solid Core PCF Based Mode Selector in MDM-Ro-FSO Transmission Systems. *Laser Phys* (2018) 28(7):1–8. doi:10.1088/1555-6611/aabd15
39. Chaudhary S, Amphawan A. High-speed MDM-Ro-FSO System by Incorporating Spiral-Phased Hermite Gaussian Modes. *Photon Netw Commun* (2018) 35(3):374–80. doi:10.1007/s11107-017-0752-6
40. Chaudhary S, Amphawan A. High-speed Millimeter Communication through Radio-Over-Free-Space-Optics Network by Mode-Division Multiplexing. *Opt Eng* (2017) 56(No. 11):116112. doi:10.1117/1.oe.56.11.116112
41. Sharma A, Chaudhary S, Thakur D, Dhasratan V. A Cost-Effective High-Speed Radio over Fibre System for Millimeter Wave Applications. *J Opt Commun* (2020) 41:177–80. doi:10.1515/joc-2017-0166
42. Chaudhary S, Chauhan P, Sharma A. High Speed 4 × 2.5 Gbps-5 GHz AMI-WDM-RoF Transmission System for WLANs. *J Opt Commun* (2019) 40: 285–8. doi:10.1515/joc-2017-0082
43. Chaudhary S, Thakur D, Sharma A. 10 Gbps-60 GHz RoF Transmission System for 5 G Applications. *J Opt Commun* (2019) 40:281–4. doi:10.1515/joc-2017-0079
44. Chaudhary S, Kapoor R, Sharma A. Empirical Evaluation of 4 QAM and 4 PSK in OFDM-Based Inter-satellite Communication System. *J Opt Commun* (2019) 40:143–7. doi:10.1515/joc-2017-0059
45. Chaudhary S, Sharma A, Chaudhary N. 6 × 20 Gbps Hybrid WDM-PI Inter-satellite System under the Influence of Transmitting Pointing Errors. *J Opt Commun* (2016) 37:99. doi:10.1515/joc-2015-0099
46. Chaudhary S, Sharma A, Neetu N. 6 X 20Gbps Long Reach WDM-PI Based High Altitude Platform Inter-satellite Communication. *System" Int J Comp Appl* (2015) 122(Issue 22):41–5. doi:10.5120/21861-5192
47. Sharma A, Chauhan P. High Speed Radio over Fiber System for Wireless Local Area Networks by Incorporating Alternate Mark Inversion Scheme. *J Opt Commun* (2021) 42:273–7. doi:10.1515/joc-2018-0084
48. Chaudhary S, Sharma A, Singh V. Optimization of High Speed and Long Haul Inter-satellite Communication Link by Incorporating Differential Phase Shift Key and Orthogonal Frequency Division Multiplexing Scheme. *Optik* (2019) 176:185–90. doi:10.1016/j.ijleo.2018.09.037
49. Chaudhary S, Tang X, Sharma A, Lin B, Wei X, Parmar A. A Cost-Effective 100 Gbps SAC-OCDMA-PDM Based Inter-satellite Communication Link. *Opt Quant Electron* (2019) 51:148. doi:10.1007/s11082-019-1864-2
50. Shakthi Murugan KH, Sharma A, Malhotra J. Performance Analysis of 80 Gbps Ro-FSO System by Incorporating Hybrid WDM-MDM Scheme. *Opt Quant Electron* (2020) 52, 1–12. doi:10.1007/s11082-020-02613-0
51. Sharma A, Malhotra J, Thappa SV, Chandhary S.. Analysis of 2 × 10 Gbps MDM Enabled Inter Satellite Optical Wireless Communication under the Impact of Pointing Errors. *Optik* (2021) 227:165250. doi:10.1016/j.ijleo.2020.165250
52. Chaudhary S, Sharma A, Tang X, Wei X, Sood P. A Cost Effective 100 Gbps FSO System under the Impact of Fog by Incorporating OCDMA-PDM Scheme. *Wireless Pers Commun* (2021) 116:2159–68. doi:10.1007/s11277-020-07784-3
53. Chaudhary S., Tang X, Sharma A, Lin B, Wei X, Parmar A. A Cost-Effective 100 Gbps SAC-OCDMA-PDM Based Inter-satellite Communication Link" Optical and Quantum Electronics, OQEL-D-18-01144. (2019). AvaliableAt: https://link.springer.com/article/10.1007/s11082-019-1864-2.
54. Chaudhary S, Wuttisittikulkij L, Nebhen J, Sharma A, Rodriguez DZ, Kumar S. Terabyte Capacity-Enabled (10 X 400 Gbps) Is-OWC System for Long-Haul Communication by Incorporating Dual Polarization Quadrature Phase Shift Key and Mode Division Multiplexing Scheme. *Plos one* (2022) 173:e0265044. doi:10.1371/journal.pone.0265044
55. Chaudhary S, Wuttisittikulkij L, Saadi M, Sharma A, Al Otaibi S, Nebhen J, et al. Coherent Detection-Based Photonic Radar for Autonomous Vehicles under Diverse Weather Conditions. *PLoS one* (2021) 16:11e0259438. doi:10.1371/journal.pone.0259438
56. Zhang C, Liang P, Nebhan J, Chaudhary S, Sharma A, Sharma B, et al. Performance Analysis of Mode Division Multiplexing-Based Free Space Optical Systems for Healthcare Infrastructure's. *Opt Quan Elect* (2021) 53: 1–14. doi:10.1007/s11082-021-03167-5
57. Sharma A, Chaudhary S, Malhotra J, Saadi M, Otaibi SA, Nebhen J, et al. A Cost-Effective Photonic Radar under Adverse Weather Conditions for Autonomous Vehicles by Incorporating a Frequency-Modulated Direct Detection Scheme. *Front Phys* (2021) 467:747598. doi:10.3389/fphy.2021.747598
58. Chaudhary S, Wuttisittikulki L, Nebhan J, Tang X, Saadi M, Otaibi SA, et al. Hybrid MDM-PDM Based Ro-FSO System for Broadband Services by Incorporating Donut Modes under Diverse Weather Conditions. *Front Phys* (2021) 506:756232. doi:10.3389/fphy.2021.756232
59. Sharma A, Malhotra J. Simulative Investigation of FMCW Based Optical Photonic Radar and its Different Configurations. *Opt Quant Electron* (2022) 54:233. doi:10.1007/s11082-022-03578-y
60. Sharoar Jahan Choyon AKM, Chowdhury R. Design of 16 × 40 Gbps Hybrid PDM-WDM FSO Communication System and its Performance Comparison with the Traditional Model under Diverse Weather Conditions of Bangladesh. *J Opt Commun* (2021). doi:10.1515/joc-2020-0247
61. Chowdhury R, Sharoar Jahan Choyon AKM. Design of 320 Gbps Hybrid AMI-PDM-WDM FSO Link and its Performance Comparison with Traditional Models under Diverse Weather Conditions. *J Opt Commun* (2021). doi:10.1515/joc-2020-0135
62. Chowdhury R, Sharoar Jahan Choyon AKM, Chowdhury SMR. Optimum Link Distance and BER Performance Investigations for BPSK RF Sub-carrier Coherent FSO Communication System under strong Turbulence. *Int J Scientific Tech Res Volume* (2020) 9(Issue 09):282–7.
63. Sharoar Jahan Choyon AKM, Chowdhury R. Performance Comparison of Free-Space Optical (FSO) Communication Link under OOK, BPSK, DPSK, QPSK and 8-PSK Modulation Formats in the Presence of Strong Atmospheric Turbulence. *J Opt Commun* (2021). doi:10.1515/joc-2019-0250
64. Chowdhury R, SharoarJahan Choyon AKM. Design and Performance Analysis of Spectral-Efficient Hybrid CPDM-CO-OFDM FSO Communication System under Diverse Weather Conditions. *J Opt Commun* (2021). doi:10.1515/joc-2021-0113

65. Ghassemlooy Z, Popoola W. Terrestrial Free Space Optical Communications. In: BSA Fares F Adachi, editors. *Mobile and Wireless Communication Network Layer and Circuit Level Design*. InTech (2010).
66. Kaushal H, Jain VK, Kar S. *Free Space Optical Communication*. USA: Springer (2017).
67. Andrews LC, Phillips RL. *Laser Beam Propagation through Random media*. Bellingham: SPIE Press Book (2005).
68. Kim I, Mcarthur B, Korevaar E. Comparison of Laser Beam Propagation at 785 and 1550 Nm in Fog and Haze for Optical Wireless Communications. *Proc SPIE Opt wireless Commun* (2006) 6303:26–37. doi:10.1117/12.417512
69. RECOMMENDATION ITU-R P.1814. (2007). Prediction Methods Required for the Design of Terrestrial Free-Space Optical Links. Report.
70. Hitam S, Suhaimi S, Noor A, Sahbudin S, Zakiah R. Performance Analysis on 16-Channels Wavelength Division Multiplexing in Free Space Optical Transmission under Tropical Regions Environment. *J Comp Sci* (2012) 8(1):145–8. doi:10.3844/jcssp.2012.145.148
71. Al-Gailani SA, Mohammad AB, Shaddad RQ. Enhancement of Free Space Optical Link in Heavy Rain Attenuation Using Multiple Beam Concept. *Optik* (2013) 124(21):4798–801. doi:10.1016/j.ijleo.2013.01.098
72. Gailani S, Mohamed A, Shaddad R, Amaludin M. Single and Multiple Transceiver Simulation Modules for Free-Space Optical Channel in Tropical Malaysian Weather. In: IEEE Business Engineering and Industrial Colloquium; 07-09 April 2013; Langkawi, Malaysia. IEEE (2013). p. 613–6.
73. Gailani S, Mohammad A, Shaddad R. Scalable Hybri WDM/Multi-beam Free Space Optical Network in Tropical Weather. In: Int. Conf. Recent Trends in Information and Communication Technologies; 02-04 September 2014; Kuala Lumpur, Malaysia. IEEE (2014). p. 12–20. doi:10.1109/ICP.2014.7002326
74. Al-Gailani SA, Mohammad AB, Shaddad RQ, Sheikh UU, Elmagzoub MA. Hybrid WDM/multibeam Free-Space Optics for Multigigabit Access Network. *Photon Netw Commun* (2014) 29:138–45. doi:10.1007/s11107-014-0482-y
75. Sahu N, Prajapti J. Optimization of WDM-FSO Link Using Multiple Beams under Different Rain Condition. *Int J Adv Res Electron Commun Eng* (2015) 4: 1125–31. doi:10.1109/ICP.2014.7002326
76. Robinson S, Jasmine S. Performance Analysis of Hybrid WDM-FSO System under Various Weather Conditions. *Frequenz* (2016) 70(9):1–9. doi:10.1515/freq-2015-0287
77. Kumar N, Teixeira A. 10 Gbit/s OFDM Based FSO Communication System Using M-Ary QAM Modulation with Enhanced Detection. *Opt Quan Elect* (2015) 48(9):1–7. doi:10.1007/s11082-015-0272-5
78. Dayal N, Singh P, Kaur P. Long Range Cost-Effective WDM-FSO System Using Hybrid Optical Amplifiers. *Wireless Pers Commun* (2017) 97(4): 6055–67. doi:10.1007/s11277-017-4826-7
79. Kaur G, Bal GS. Performance Analysis of SAC-OCDMA in Free Space Optical Medium Using DDW Code. *Optik* (2017) 133:36–42. doi:10.1016/j.ijleo.2016.12.057
80. Sharma V, Lumba M, Kaur G. Severe Climate Sway in Coherent CDMA-OSSB-FSO Transmission System. *Optik* (2014) 125:5705–7. doi:10.1016/j.ijleo.2014.06.088
81. Kakati D, Arya SC. Performance of 120 Gbps Single Channel Coherent DP-16-QAM in Terrestrial FSO Link under Different Weather Conditions. *Optik* (2019) 178:1230–9. doi:10.1016/j.ijleo.2018.10.035

Conflict of Interest: The authors declare that the research was conducted in the absence of any commercial or financial relationships that could be construed as a potential conflict of interest.